Journal: Energy&Fuels

Special Issue: In Honor of Michael J. Antal

DOI: 10.1021/acs.energyfuels.6b01030

Energy Fuels 2016, 30, 8019−8030

Comprehensive compositional study of torrefied wood and herbaceous materials by chemical analysis and thermoanalytical methods

Eszter Barta-Rajnai*[1], Emma Jakab[1], Zoltán Sebestyén[1], Zoltán May[1], Zsolt Barta[2], Liang Wang[3], Øyvind Skreiberg[3], Morten Grønli[4], János Bozi[1], Zsuzsanna Czégény[1]

*rajnai.eszter@ttk.mta.hu

[1]Institute of Materials and Environmental Chemistry, Research Centre for Natural Sciences, Hungarian Academy of Sciences, Budapest, Hungary

[2]Department of Applied Biotechnology and Food Science, Budapest University of Technology and Economics, Budapest, Hungary

[3]SINTEF Energy Research, Trondheim, Norway

[4]Department of Energy and Process Engineering, Norwegian University of Science and Technology (NTNU), Trondheim, Norway

ABSTRACT

In this work the torrefaction of three biomass materials: black locust wood, wheat and rape straw was studied at various temperatures: 200, 225, 250, 275 and 300 °C. The thermal stability and the

formation of the decomposition products of the untreated and treated samples were measured by TG/MS method. The degree of hemicellulose and cellulose decomposition during torrefaction at different temperatures were characterized by compositional analysis of the torrefied and untreated samples. The cellulose, hemicellulose and Klason-lignin contents of the raw and torrefied biomass samples were determined by acidic hydrolysis and subsequent HPLC analysis. The inorganic ion contents of the untreated samples were measured by ICP-OES method. The joint evaluation of the results obtained by various analytical methods revealed that the acidic side groups of hemicellulose were partially split off, while the main mass of hemicellulose did not degrade at 225 °C torrefaction temperature. About 40% of hemicellulose degrades at 250 °C torrefaction temperature and the remainder decomposes at higher temperature. Although hemicellulose has different chemical structure in the hardwood and the straws, no significant differences were observed in the thermal stability of hemicelluloses in the three studied samples. Taking into consideration the significantly higher alkali ion content of the straw samples it was concluded that the alkali ion content of the samples did not modify the thermal stability of hemicellulose. Statistical analysis (PCA) have been used to present correlations between the torrefaction temperature, chemical composition and thermal parameters of the samples. The PCA calculations revealed substantial changes in the chemical composition and thermal properties of biomass materials as a result of torrefaction at 275-300°C temperatures.

KEYWORDS: Torrefaction, Wood, Herbaceous biomass, Cellulose, Hemicellulose, Lignin, Thermogravimetry, Mass spectrometry, Principal component analysis

ABBREVIATIONS

BL	Black locust
RS	Rape straw
WS	Wheat straw
BLU	Untreated black locust
BL 200	The torrefied black locust obtained from torrefaction at 200 °C
HHV	Higher heating value
MC	Moisture content
VM	Volatile matter
FC	Fixed carbon
DTG_{max}	Maximum value of the DTG curves
T_{peak}	Temperature of the maximum of the DTG curves
$T_{1\%}$	Temperature belonging to the 1% mass loss of the dried samples
T_{start}	Extrapolated temperature of the beginning of decomposition (on the DTG curve)[1]
T_{end}	Extrapolated temperature of the end of cellulose decomposition (on the DTG curve)[1]
Char	Char residue at 950 °C temperature
PCA	Principal component analysis

1. INTRODUCTION

Biomass is a primary type of renewable energy source which is one of the most abundant energy sources on the Earth. In energetic utilization, the unfavorable properties of the untreated biomass are the following: high moisture content, low calorific value, low energy density, high oxygen content, and hydrophilic nature. The transportation and storage are costly due to the low density of biomass

materials, espeically for those derived from agricultural sector. The unfavorable properties of raw biomass can be improved by torrefaction, which is a thermal treatment between 200 and 300 °C in an inert atmosphere for the partial conversion of biomass. [1-3] The torrefaction process can be classified into light, mild and severe torrefaction, where the temperatures are approximately 200-235 °C, 235-270 °C and 270-300 °C, respectively. During torrefaction the moisture content of biomass is removed and the acidic functional groups of the hemicellulose component are cleaved.[4-5] These reactions result in the increase of the calorific value and the higher stability against biodegradation of the torrefied biomass leading to reduced transportation and storage costs.[6-8]

Several types of biomass materials have been torrefied including agricultural[9-15] and forestry by-products.[16-20] Torrefied wood and straw in the form of pellets can be directly co-fired with coal in a relatively high ratio hereby utilizing the processing infrastructures at existing coal power plants. As a consequence of the difference in the relative amount of cellulose, hemicellulose, lignin, and extractives, the woody and herbaceous materials behave differently during thermal decomposition.[21-22] Several factors may affect the thermal decomposition of lignocellulosic materials. The alkali ions have significant impact on the thermal degradation mechanisms of cellulose,[1,23–30] the depolymerization reaction is hindered and the fragmentation reactions are promoted leading to the decreased decomposition temperature and the increased char yield. Sebestyén et al.[31] concluded that the concentration of the potassium and sodium ions in the hemp sample determines the effect of alkali ions to a great extent. The largest alteration of the TG/MS parameters was detected in the 0–0.2 mmol g^{-1} concentration range of the alkali ions. Of all the inorganic components of biomass, potassium has the biggest influence on the thermal behavior.[23-25] The inorganic ions modifies also the decomposition of lignin,[1,32-35] although to a lesser extent than in case of cellulose.

Thermal analysis and pyrolysis are useful methods to reveal differences in the composition of biomass samples without separating the components.[35-36] The coupled techniques, such as thermogravimetry/mass spectrometry[37-39] and thermogravimetry/ Fourier transform infrared spectrometry[40-41] can provide detailed information about the volatile decomposition products of the samples.

In this work the torrefaction of black locust wood (*Robinia pseudoacacia*), wheat straw (*Triticum aestivum*) and rape straw (*Brassica napus*) was studied, which are typical biomass products or by-products in Hungary. Black locust wood is native to the southeastern United States, but it is widespread in Europe, as well. It can be a promising biomass for future energy production because of its high growth rate and favorable fuel characteristics, such as low ash content and high heating value. Straw is a low value by-product of the agricultural industry and it is available in large quantities.

The purpose of this work is to study the thermal behavior of torrefied woody and herbaceous biomass materials and understand the chemical changes which take place during torrefaction at different temperatures. The thermal stability and the formation of the volatile products of the untreated and treated samples were studied by thermogravimetry/mass spectrometry (TG/MS). The chemical composition (cellulose, hemicellulose and lignin content) of the untreated and torrefied samples was determined by a two-step acid hydrolysis. The obtained thermoanalytical and compositional data were evaluated by statistical analysis with the goal to present correlations between the temperature of the torrefaction pretreatment, the thermal behavior of the wood and herbaceous samples and the chemical composition of the samples.

2. EXPERIMENTAL SECTION

2.1 Materials. A black locust wood and two herbaceous biomass materials (rape straw and wheat straw) were selected for the torrefaction study. The raw samples were dried in an oven at 105 °C for 8 hour to obtain samples of similar moisture content for the experiments, and to avoid biodegradation during storage. In spite of the thorough drying the samples had about 6% moisture content prior to the torrefaction experiments (based on TG measurement), which can be explained apparently by the moisture uptake during sample handling. The untreated samples were ground to <1 mm particle size by a cutting mill.

2.2 Torrefaction. The torrefaction experiments were performed in nitrogen atmosphere in a horizontal tube furnace. About 12 g samples were treated in a glass boat of 200 mm long. The flow rate of the nitrogen gas was set to a relatively low value of 20 ml min^{-1} in order avoid the removal of the smaller particles from the boat. The torrefaction experiments were performed at 200 °C, 225 °C, 250 °C, 275 °C and 300 °C temperatures using isothermal period of one hour.

2.3 Proximate and ultimate analysis. The samples were characterized before and after torrefaction, using proximate analysis and elemental (ultimate) analysis. The moisture and volatile content of the untreated and torrefied biomass samples were determined by thermogravimetry heating the samples from room temperature up to 950 °C. The amount of ash was measured using the standard method proposed by National Renewable Energy Laboratory (NREL/TP-510-42622) applying 550 °C ashing temperature. The fixed carbon content was determined by difference. The carbon and hydrogen contents of the untreated and torrefied biomass samples were measured by an elemental analyzer. The oxygen content was determined by difference. Three parallel proximate and ultimate analyses were

performed to validate repeatability of the results, which was found to be quite satisfactory with max. ±1% standard deviation.

2.4 Higher heating value determination. The higher heating value (HHV) was determined using an automatic IKA C 5000 bomb calorimeter. The combustion of about 0.5 g dried sample in pure oxygen atmosphere was performed under 30 bar pressure. Benzoic acid calibration was applied to determine the heat capacity of the calorimeter. All heating values were calculated from the averages of three replicates.

2.5 Inductively coupled plasma-optical emission spectroscopy (ICP-OES). The ashing of 2 g biomass samples was carried out in a furnace at 550 °C according to CEN/TS 14775:2004 EU standard method. The ashes were fused with a fusion blend ($Li_2B_4O_7$:$LiBO_2$, 2:1) at 920 °C and digested by 25 mL 33% nitric acid. The sodium, potassium, calcium and silicon contents of the untreated samples were measured by a Spectro Genesis ICP-OES (Spectro Analytical Instruments) with axial plasma observation.

2.6 Carbohydrate and Klason lignin content determination. The contents of carbohydrates were determined according to the method of Sluiter et al.[42] applying slight modifications. The milled samples were dried at 40 °C for 1 day. The untreated and torrefied biomass samples were treated in a two-step acid hydrolysis with 72% H_2SO_4 for 2 hours at room temperature, and then with 4% H_2SO_4 for 1 hour at 121 °C. The obtained suspensions were filtered and washed with distilled water through G4 glass filter crucibles. The sugar concentrations (glucose, xylose and arabinose) of the filtered supernatants were analyzed with high performance liquid chromatography (HPLC) using an Agilent 1260 system with an Hi-Plex H column (Agilent, CA, USA) at 65 °C. An eluent of 5 mM H_2SO_4 was used at a flow rate of 0.5 mL min^{-1}. The solid residues obtained after washing were dried at 105 °C

until constant weight. The dried residues consisted of acid-insoluble organics and acid-insoluble ash. The amounts of total ash and acid-insoluble ash were determined by ashing the sample at 550 °C for 5 hours until the sample weight was constant.[43] The Klason lignin content was calculated by subtracting the acid insoluble ash content from the acid insoluble residue content. All experimental data were determined using three replicates.

2.7 Thermogravimetry/mass spectrometry (TG/MS). The TG/MS experiments were carried out using a modified Perkin-Elmer TGS-2 thermobalance connected to a Hiden HAL quadrupole mass spectrometer. About 5 mg samples were heated from 25 to 950 °C at a rate of 20 °C min^{-1} in a platinum sample pan. The evolved products were led through a glass lined metal capillary heated at 300 °C using argon carrier gas at a flow rate of 140 mL min^{-1}. The high flow rate minimizes the time delay between the measurements of the mass in the thermobalance and the ion intensities in the mass spectrometer. The ion source of the mass spectrometer was operated at 70eV electron energy. The mass range of 2-150 Da was scanned. The ion intensities were normalized to the sample mass and to the intensity of the ^{38}Ar isotope of the carrier gas.

2.8 Principal component analysis (PCA). Due to the large number of samples and experimental data a chemometric tool, principal component analysis (PCA) using Statistica 12 software (StatSoft, Inc. Tulsa, Oklahoma, USA), was employed. PCA has been applied to find correlations between TG data, energy content and the chemical composition of the samples as well as to reveal further correlations between the thermogravimetry/mass spectrometry data of the untreated and torrefied samples. PCA is a technique, which decreases the data dimensionality and makes pattern visualization by converting the original measured data into new uncorrelated variables (principal components).[44] The principal components (Factors) are the linear combinations of the original measured variables. The principal components (Factors) explain different percentages of the total

variance; generally two or three Factors are enough to describe the differences and similarities between the samples. The results can be presented in the score plots, which place the samples in the space of two Factors. Factor loadings show the correlation between the original data and the principal components.

3. RESULTS AND DISCUSSION

3.1 Characterization of untreated and torrefied biomass samples. The solid yield, the proximate and ultimate analysis data and the energy content of the untreated and torrefied samples are shown in Table 1. During torrefaction the moisture content and volatiles release from the sample resulting in a decrease of the sample mass. Up to the temperature of 250 °C, the yield of the solid residue was quite similar for the three investigated samples. Comparing the results obtained at 250 °C and 275 °C it can be established that a significant decrease of the solid yield occurred in rape and wheat straw samples (15 and 20%, respectively), while the solid yield was reduced to a lesser extent in black locust wood (11%). This observation indicates a higher degree of decomposition of herbaceous samples at about 275 °C.

The proximate analysis data of the torrefied samples shows that the moisture content and volatile matter decreased, while the ash and fixed carbon content increased in the samples prepared at higher torrefaction temperature, due to the progress of the thermal decomposition. Black locust wood had higher volatile matter content and lower fixed carbon yield than wheat and rape straw samples, prepared under the same torrefaction conditions.

The ultimate analysis shows that the increasing torrefaction temperature increased the carbon content and reduced the oxygen and hydrogen content of the torrefied materials. The calorific value of the torrefied samples increased with the increasing temperature. Torrefaction at 225 °C increased the HHV of the samples by at least 3.5% in comparison with the value of the untreated samples (17.6-

18.2 MJ kg^{-1}). Torrefaction at 275 °C resulted in an increase of 19-27% of the HHV. All of the proximate and ultimate analysis data as well as the calorific values verify the gradual thermal decomposition of the biomass samples by increasing temperature.

Principal component analysis has been performed to obtain statistical correlations between the solid yields, the energy contents and the proximate and ultimate analysis data (Table 1). The PCA results can be found in Figure S1 in the supporting information.

The alkali ion contents of the untreated samples have been determined using ICP-OES technique. Table 2 shows the most important data of the ICP-OES results of the untreated black locust, rape straw and wheat straw samples. As the data illustrate, wheat and rape straw samples have an order of magnitude higher K^+ content than the wood sample. Furthermore, Na^+, Ca^{2+} and Si contents of the two straw samples are also significantly higher comparing to the black locust sample

Table 1. Characterization of the Studied Samples

Sample	Solid yield (%)	Proximate analysis (% m/m, as received)				Ultimate analysis (% m/m, dry basis)			HHV (MJ kg^{-1})
		MC	VM	Ash	FC	C	H	O	
Black locust									
BL U	100	6.08	77.85	1.75	14.32	48.10	4.74	45.41	18.17
BL 225	87	3.25	76.87	1.91	17.97	50.59	3.45	44.05	19.35
BL 250	79	3.23	69.79	2.16	24.82	52.77	4.39	40.68	20.38
BL 275	68	3.42	65.83	2.92	27.83	53.05	8.59	35.44	21.61
BL 300	49	3.78	56.34	4.2	35.68	60.65	8.30	26.85	27.87
Rape straw									
RS U	100	7.16	71.16	6.04	15.64	46.3	5.46	42.2	17.68
RS 225	85	4.62	68.99	6.36	20.02	47.23	5.22	41.19	18.84
RS 250	76	4.11	66.01	7.26	22.62	48.86	5.79	38.09	20.21
RS 275	61	4.57	53.61	9.36	32.46	52.38	5.14	33.12	22.46
RS 300	47	3.76	40.73	11.84	43.67	60.84	4.81	22.51	25.08
Wheat straw									
WS U	100	5.58	70.55	5.68	18.19	49.38	4.23	41.04	17.87
WS 225	89	3.68	69.69	5.80	20.83	47.68	4.10	42.42	18.48
WS 250	80	3.48	66.20	6.92	23.40	48.49	6.62	38.11	19.15
WS 275	60	3.53	54.84	9.28	32.34	56.12	4.63	29.97	21.73
WS 300	44	2.37	38.12	12.52	46.98	62.28	4.83	20.37	26.42

Table 2. The Most Important Inorganic Components of the Studied Samples

Sample	Inorganic content (% m/m dry basis)				
	Si	K^+	Na^+	Ca^{2+}	Mg^{2+}
Black locust	* N. D.	0.12	* N. D.	0.085	0.017
Rape straw	0.03	1.86	0.072	0.503	0.158
Wheat straw	1.07	1.69	0.008	0.137	0.077

* N. D.: Not determined, below the detection limit

3.2 Carbohydrate and lignin content. The compositional analysis of each studied biomass was performed in order to understand better the thermal conversion process during torrefaction. The results are presented in Figure 1. The glucan content of the samples mainly characterizes the cellulose component of biomass, while the sum of the xylan and arabinan content represents the hemicellulose fraction. The Klason lignin is defined as the acid insoluble residue content of the samples without the acid insoluble ash content. The fraction denoted "other" in Figure 1 represents the sum of the unquantified components and includes extractives, acid soluble lignin and acid soluble minerals. To compare the degradation degree of cellulose, hemicellulose and lignin in the torrefied samples, one have to take into consideration the mass loss during the torrefaction experiment as well. Therefore, Figure 1 also shows the mass loss during the torrefaction at the different temperatures.

The comparison of the chemical composition of the three untreated samples shows that black locust has the highest Klason-lignin content (25.7%), while wheat straw has the highest hemicellulose (23%) content. The lignocellulose content (sum of cellulose, hemicellulose and lignin) of black locust and wheat straw samples is around 76%, while that of the untreated rape straw is only 66%. The reason could be the higher amount of extractive compounds and the higher acid soluble mineral content of the rape straw sample. The later assumption is supported by the highest alkali and alkali earth ion content of the rape straw sample as shown in Table 2.

During torrefaction the lignocellulose materials decompose to different degrees depending on the applied temperature. The variation of the amount of glucan, xylan and arabinan in the torrefied samples (see Figure 1) reflects the changes in the proportion of cellulose and hemicellulose in the samples. The decreasing carbohydrate yields indicate the progress of the thermal decomposition of hemicellulose and cellulose during torrefaction at various temperatures.

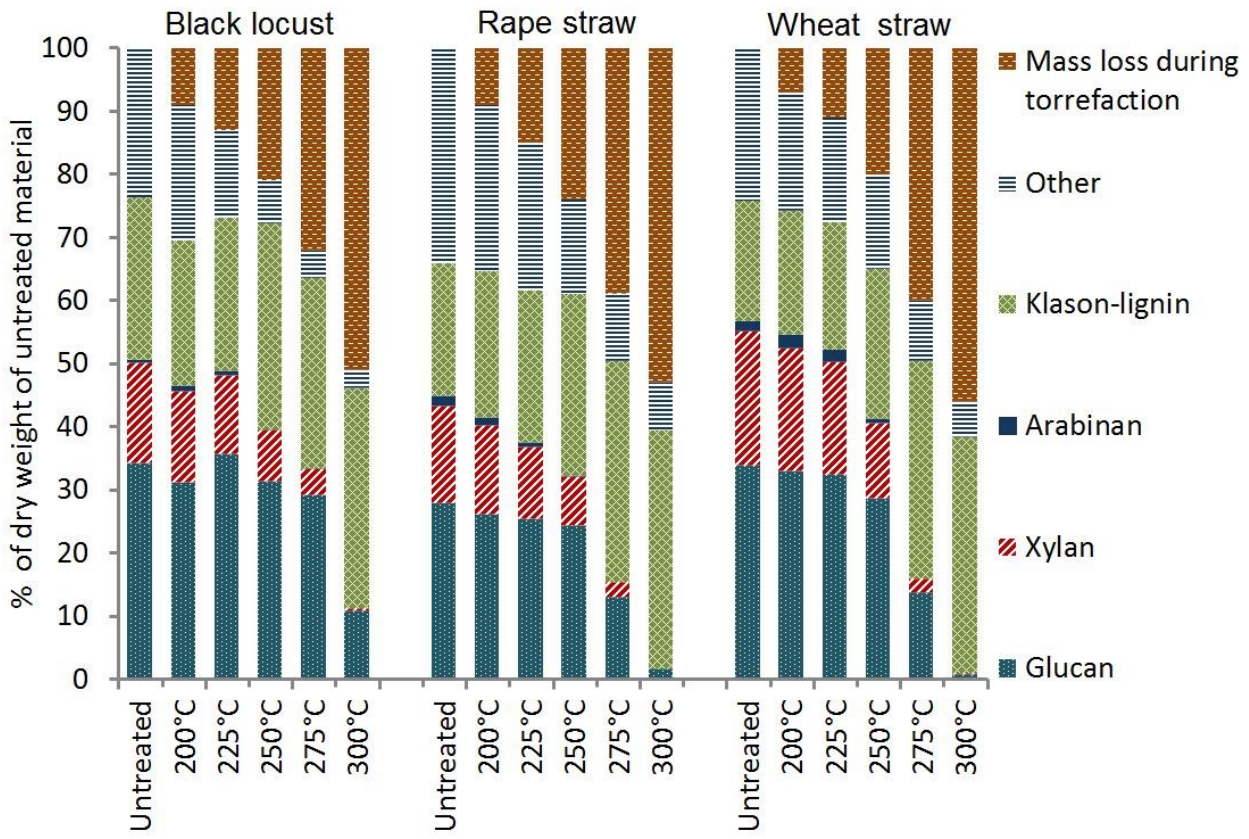

Figure 1. Composition of the untreated and torrefied black locust wood, rape straw and wheat straw (calculated on dry basis).

As the results present, hemicellulose (measured as the sum of arabinan and xylan) is the thermally least stable component of the lignocellulose fraction during torrefaction. The hemicellulose content of the torrefied samples is slightly decreased up to 225 °C for each studied samples. The samples torrefied at 250 °C have about half of the hemicellulose content of the untreated sample for each biomass. At higher torrefaction temperatures the relative amount of the hemicellulose drastically decreases, and only traces of hemicellulose were measured in the samples torrefied at 300 °C. The changes in the relative amount of hemicellulose show similar tendency as a function of torrefaction temperature for each sample, indicating that the thermal stability of hemicellulose is similar in the

studied wood and herbaceous samples. Hence, it can be concluded that the alkali ion content of the samples does not modify significantly the thermal stability of hemicellulose.

The variation of the cellulose content in the untreated and torrefied samples is demonstrated by the amounts of glucan (Figure 1). As the bar diagram shows, the cellulose content of black locust wood does not decrease considerably up to 275 °C torrefaction temperature. In case of the two herbaceous samples, the degradation of cellulose is significant at this temperature; the relative decrease is almost 50% in both cases. At 300 °C torrefaction temperature, about 60% of the cellulose content of black locust decomposes, while cellulose almost disappears from rape and wheat straw samples. On the basis of this observation it can be concluded that the thermal stability of cellulose in the herbaceous samples is lowered by about 25 °C compared to wood. The herbaceous samples have more than an order of magnitude higher alkali ion contents than wood. The catalytic effect of alkali ions on the thermal decomposition of cellulose is known[23-30]. The results obtained for the cellulose content of the torrefied samples confirm that the alkali ions have catalytic effect on cellulose decomposition even at the low temperatures used in torrefaction.

As Figure 1 presents, increasing the torrefaction temperatures resulted in a significant increase in the measured Klason-lignin content of the samples. Besides the acid-insoluble lignin, the Klason-lignin contains all acid insoluble components of the sample excluding ash. During the thermal treatment some parts of the extractives, cellulose, hemicellulose and acid soluble lignin were probably transformed into acid insoluble carbonaceous products by cross-linking and charring reactions. The increasing torrefaction temperature favors these reactions, resulting in the increased Klason-lignin value at higher temperatures.

3.3 Thermogravimetric results. The thermogravimetric (TG) and derivative thermogravimetric (DTG) curves of the samples are shown in Figure 2. Comparison of the curves shows that the shape

of the TG and DTG curves of rape straw and wheat straw samples are rather similar, while black locust wood behaves differently during thermal decomposition. It is described in the literature[23-30] that the difference between the behavior of wood and herbaceous samples is partly due to the different alkali ion contents, which have significant effect on the thermal properties of cellulose. The different thermal behavior of the torrefied woody and herbaceous biomass materials can also be interpreted by their different inorganic ion contents. In addition, the relative amounts of alkali ions further increased in the samples during the torrefaction.

The evaporation and decomposition of extractives in the untreated samples are visible on the DTG curve as a broad shoulder starting approximately at 180 °C. The higher weight loss of untreated rape straw compared to wheat straw and black locust (Figure 2 a, b) between 200 and 300 °C indicates the highest extractive content of this sample. During torrefaction at 225 °C the extractive content of the samples mostly evaporated, therefore the above mentioned difference disappeared from the TG and DTG curves of rape straw (Figure 2 c, d) and the weight loss curves of the three torrefied biomass overlap up to 300 °C. This observation is in accordance with the results of compositional analysis, where higher amount of extractives and/or acid soluble inorganics was determined in the untreated rape straw sample (see “other” component in Figure 1) than in the other biomass samples studied.

The main DTG peak of the untreated samples (Figure 2 b) can be explained by the decomposition of cellulose. The characteristic shoulder on the DTG curve of the untreated black locust sample (Figure 2 b) up to 350 °C represents the decomposition of hemicellulose. In case of herbaceous samples the hemicellulose shoulder is not pronounced because the cellulose decomposition shifted to lower temperature due to the catalytic effect of the high amounts of alkali ions. O-Acetyl-4-O-methylglucuronoxylan is the main building block of hemicellulose in hardwood species. In herbaceous biomass, arabinoxylans are the dominant hemicellulose polysaccharides. As the

compositional analysis data demonstrates (Figure 1), the hemicellulose content of the samples did not degrade during torrefaction at 225 °C. Accordingly, the obtained DTG curve of black locust torrefied at 225 °C (Figure 2 d) has a significant shoulder representing the decomposition of hemicellulose. After torrefaction at 250 °C (Figure 2 e, f), the characteristic shoulder on the DTG curve of the wood sample disappeared indicating that the hemicellulose decomposed or its structure changed as a result of the torrefaction. The results of the acidic hydrolysis revealed, that about 40% of the hemicellulose content decomposed during the torrefaction at 250 °C temperature. The significant hemicellulose content of the samples torrefied at 250 °C contradicts the disappearance of the hemicellulose shoulder from the DTG curve. These results can be explained by the assumption that the thermally most labile functional groups (e.g., acetyl groups) of hemicelluloses were split off under torrefaction; therefore the remaining hemicellulose chains became more stable and decomposed in a similar temperature range as cellulose.

Regarding the cellulose component of the torrefied biomass samples, the thermogravimetric curves confirm the results of the compositional analysis. Low-temperature torrefaction has only a small effect on the amount of cellulose. After torrefaction at 275 °C (Figure 2 g, h), the maximal rate of thermal decomposition of both straw samples decreased by about 50% indicating the high degree of cellulose decomposition during the torrefaction. In case of the black locust sample, torrefaction at 275 °C still did not affect significantly the cellulose content. These observations also indicate the catalytic effect of alkali ions on the decomposition of cellulose, and are in agreement with the results of the compositional analysis. After torrefaction at 300 °C, the DTG curve of black locust is significantly reduced, but still with some cellulose content extant; while the DTG curves of wheat straw and rape straw have (Figure 2 j) a wide and flat shape, indicating the almost complete decomposition of cellulose. The lignin decomposes at a low rate in a wide temperature range from 250 to 600 °C, hence it does not have a separated DTG peak. Lignin is a complex cross-linked methoxyphenol-based

polymer built of so called monolignol subunits: p-coumaryl alcohol, coniferyl alcohol, and sinapyl alcohol. The lignin of the herbaceous plants is composed of all three types of monolignols, while the hardwood lignin is built of only coniferyl alcohol and sinapyl alcohol. The lignin and the alkali ion contents of the samples have considerable effect on the char yield of biomass. Lignin produces about 30% char[33,45], whereas the decomposition of cellulose and hemicellulose leads to only about 5% and 5-10% solid residue, respectively. The inherent alkali ion content of biomass changes the thermal decomposition mechanism: higher char yield and increased amount of gaseous products are formed with increasing alkali ion content.[31]

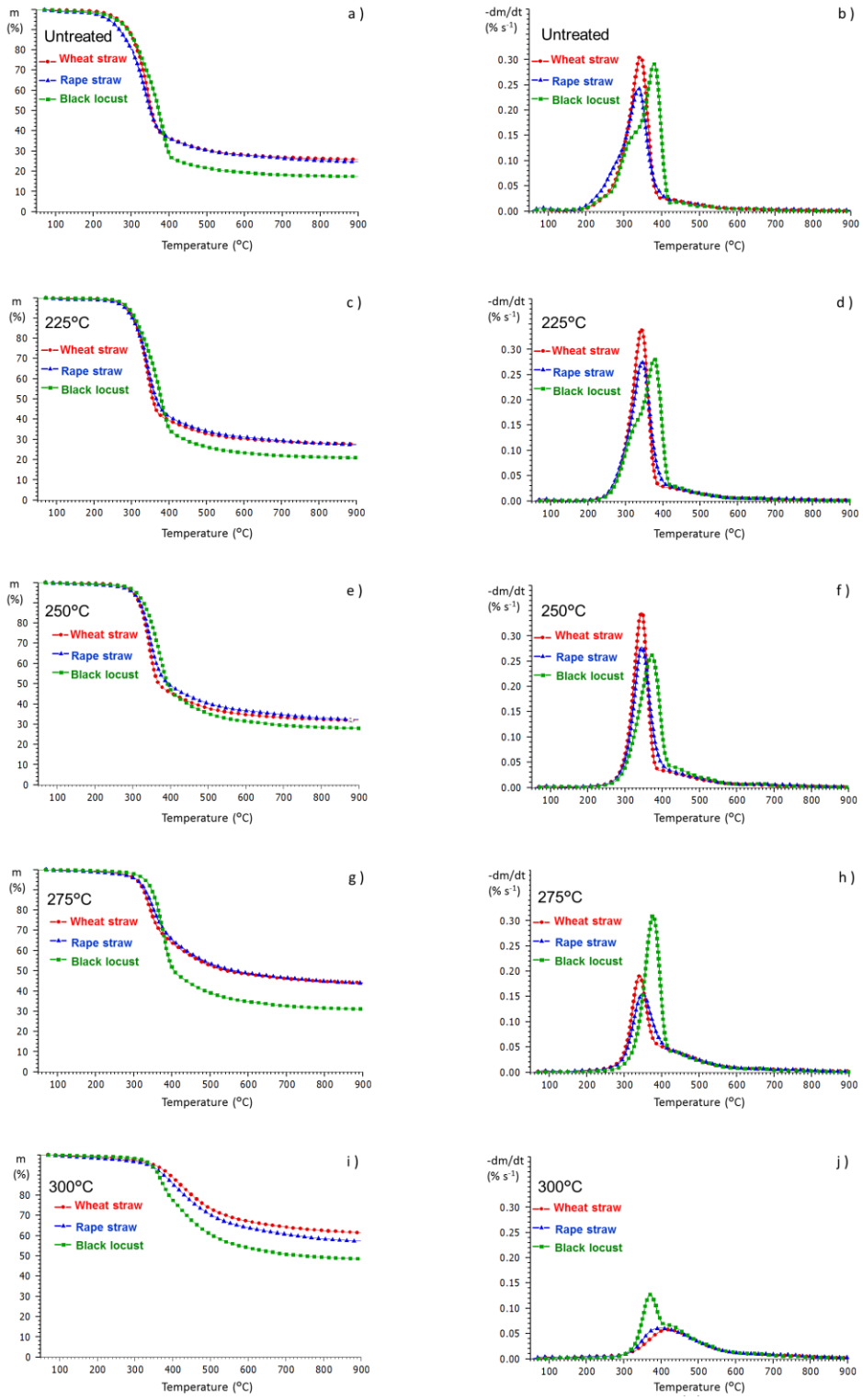

Figure 2. TG and DTG curves of black locust wood, rape straw and wheat straw before and after the various torrefaction treatments.

3.4 Principal component analysis based on the calorific values, TG and chemical composition data. The TG parameters (T_{peak}, DTG_{max}, T_{start}, $T_{1\%}$, T_{end}, char yield), glucan, xylan and lignin contents, and higher heating values have been used in the calculation as input data to illustrate the differences and similarities between the untreated and the torrefied biomass samples (Table 1, Figure 1 and 2). Besides the extrapolated T_{start} value, $T_{1\%}$ was also used for the description of the beginning of the decomposition, which represents the temperature of 1% mass loss after the release of the adsorbed water. T_{start} denotes the start of hemicellulose decomposition, while T_{end} shows the end of cellulose decomposition. In the PCA calculation the first principal component (Factor 1) characterizes 67.26%, while the second and third principal components (Factor 2 and Factor 3) describe 14.67% and 9.86% of the total variance, respectively. These three factors describe adequately the main differences between the samples. The score plot for Factor 1 and Factor 2 (Figure 3 a) shows that the black locust (BL), rape straw (RS) and wheat straw (WS) samples can be seen in different parts of the plot. The first principal component differentiates the untreated, the mildly and severely torrefied samples. As a function of the second principal component, the herbaceous samples are found in the upper, and the woody samples in the lower, part of the score plot. This difference is apparently due to the different cellulose, hemicellulose, lignin, and extractive content of the samples; which is reflected in the different thermal behavior of woody and herbaceous materials.

The loading plot for Factor 1 and Factor 2 (Figure 3 b) shows that the values of glucan and xylan content and DTG_{max} data correlate negatively with the higher heating value (HHV), lignin content, char yield and T_{start} and $T_{1\%}$ data. Factor 1 is composed of mainly these parameters and mostly separates the samples as a function of the torrefaction temperature. Figure 3 a shows that the herbaceous samples torrefied at 275 and 300 °C are separated, essentially indicating the severe decomposition. T_{peak} and T_{end} data contribute mainly to Factor 2, these parameters describe the cellulose decomposition. Untreated black locust (hardwood) and wheat straw have similar cellulose

content (approximately 34%); however, straw samples have more than an order of magnitude higher K^+ and Na^+ content than black locust (Table 2). Due to the alkali catalysis, the characteristic temperatures of cellulose decomposition of the herbaceous samples shift to lower temperatures. Mainly this effect is reflected in Factor 2.

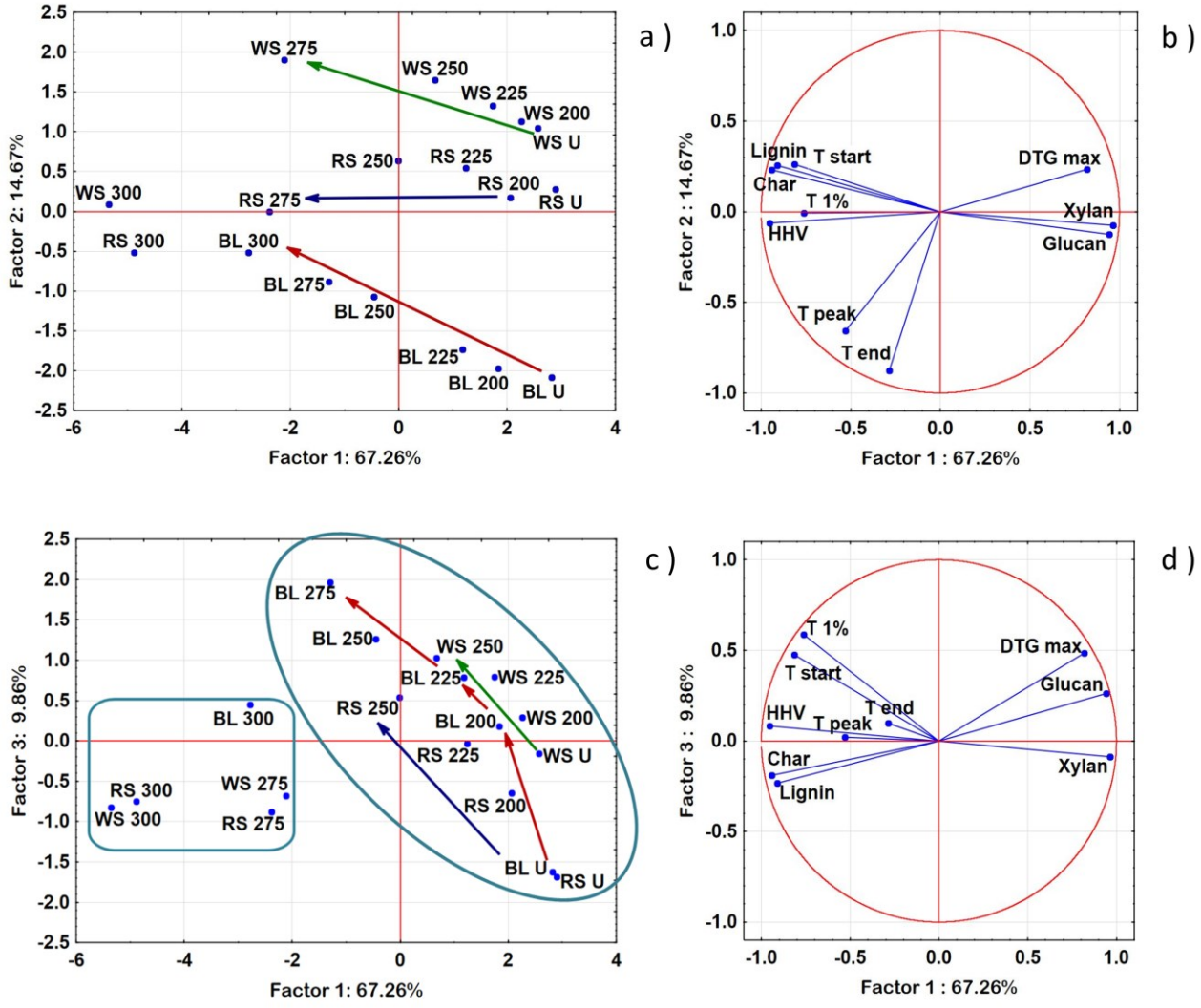

Figure 3. Principal component analysis (a, c) score and (b, d) loading plots based on the calorific values, thermogravimetric and chemical composition data. The score plots (a, c) represent the samples in the space defined by the Factors. Factor loadings (b, d) show the correlation between the

original variables and the Factors. The arrows show the direction of the variation of the samples with increasing torrefaction temperatures. WS: wheat straw, RS: rape straw, BL: Black locust wood

Factor 3 describes almost 10% of the total variance. The loading plot (Figure 3 d) shows that the values of $T_{1\%}$, T_{start}, cellulose content and DTG_{max} contribute to Factor 3 and 1, as well. $T_{1\%}$ and T_{start} can be attributed to the hemicellulose decomposition in untreated and mildly-treated samples, while after severe torrefaction, i.e., after the decomposition of hemicellulose, these parameters belong to the cellulose decomposition. The samples formed two groups as a function of Factor 1 and 3 as shown in Figure 3 c. The severely torrefied samples are separated from the untreated and mildly torrefied biomass samples. As mentioned above, the maximum rate of thermal decomposition (DTG_{max}) of straw samples decreased by half between the torrefied samples at 250 °C and 275 °C, while the DTG_{max} data of black locust wood only differ significantly between the samples treated at 275 °C and 300 °C. It was found that the hemicellulose and cellulose content of the studied samples strongly decreased from 250 °C to 300 °C (see Figure 1). At the severe torrefaction temperatures (275-300 °C), the chemical composition of the samples significantly changed during torrefaction, therefore the thermal properties of the samples were altered to a greater extent in this temperature range.

3.5 TG/MS results. The evolution profiles of the most characteristic decomposition products of the untreated and torrefied black locust and wheat straw samples are presented in Figure 4 and 5. The curves for the individual species released from black locust wood and wheat straw are plotted in the

same scale in each of the figures. The pattern of the ion intensity curves of rape straw is very similar to that of wheat straw; hence it is not presented here.

Figure 4 shows the evolution of the main permanent gases and water from black locust wood and wheat straw. Relatively large amounts of water and carbon dioxide are produced during the thermal decomposition of the samples due to the various types of hydroxyl and other oxygen-containing functional groups in the natural polymers (cellulose, hemicellulose, and lignin). The higher temperature charring processes are characterized by the evolution hydrogen (*m/z* 2) and methane (*m/z* 16). Figure 5 shows the evolution of some characteristic organic volatile products and fragment ions from the black locust wood and wheat straw samples. Formaldehyde (*m/z* 30) forms during the thermal decomposition of cellulose, hemicellulose and lignin, as well. The release of methanol can be monitored at *m/z* 31. Furthermore, *m/z* 31 is the main fragment ion of hydroxyacetaldehyde, which is an important product of cellulose decomposition. The evolution curve at *m/z* 60 ion may represents either acetic acid released mostly from the acetate groups of hemicellulose or hydroxyacetaldehyde formed mainly during cellulose decomposition. The *m/z* 27 ion is a typical fragment ion of hydrocarbons.

The moisture content (*m/z* 18 in Figure 4) releases from the samples up to 120 °C. During torrefaction the moisture content of the sample were released; however, during sample handling the torrefied sample can take up some water from the air depending on the degree of hydrophilicity of the torrefied sample. The moisture content of the torrefied straw samples is higher than that of the torrefied wood samples, which may be explained by the higher inorganic ion content, therefore the more hydrophilicnature of the torrefied straw samples.

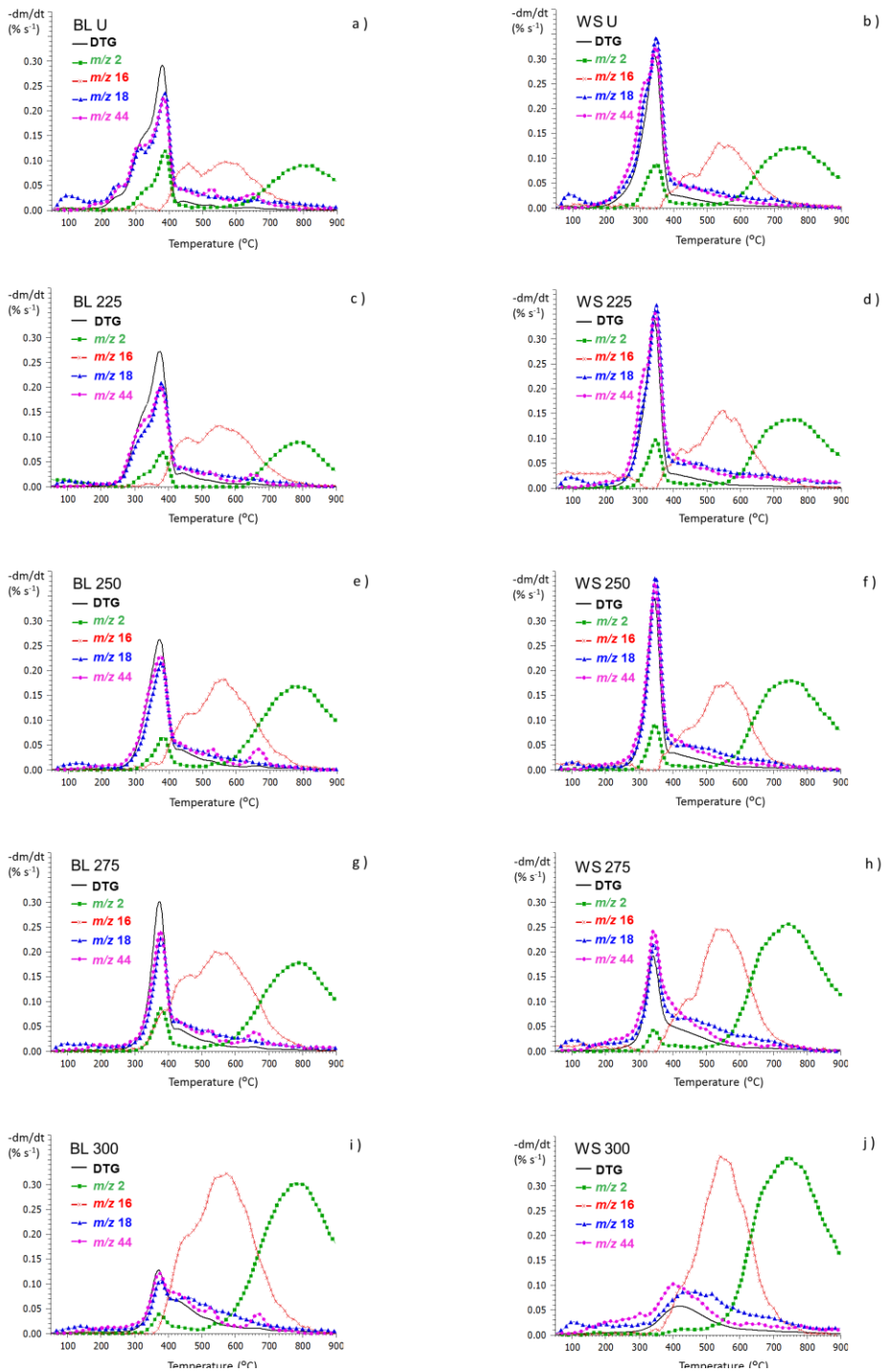

Figure 4. DTG curves and the evolution profiles of the main permanent gases and water from black locust wood and wheat straw. (*m/z* 2, hydrogen; *m/z* 16, methane; *m/z* 18, water; *m/z* 44, carbon dioxide)

The evolution of water, carbon dioxide, formaldehyde and methanol (Figure 4 a, b and 5 a, b) in the temperature range of 200-250 °C reveals the thermolysis of extractives and scission of lignin side groups from the untreated samples. These processes start at around 200 °C and the significant shoulder at 230 °C on the DTG and ion curves of untreated black locust can be attributed to the decomposition of extractives.[46] During 1 hour thermal pretreatment at 225 °C the extractive content of the sample decomposed, therefore the shoulder at 230 °C disappeared from the torrefied samples (Figure 4 c and 5 c).

The characteristic peaks or shoulders of formaldehyde, acetic acid, methanol, carbon dioxide and water in the temperature range of 280-350 °C of the untreated wood sample (Figure 4 a and 5 a) represent the decomposition of hemicellulose. In case of the herbaceous samples the shoulder is not pronounced because the cellulose decomposition shifts to lower temperature due to the higher alkali ion content. The evolution of acetic acid and carbon dioxide indicates the scission of the acidic groups from hemicellulose. The composition analysis revealed that the hemicellulose content of the samples does not decrease during thermal treatment at 225 °C. However, the ion intensities of the significant decomposition products of hemicellulose slightly decreased in case of the wood sample (Figure 4 c and 5 c). This observation may point to the somewhat modified structure (e.g. scission of the most labile acidic groups) as a result of torrefaction at 225 °C. The TG/MS curves of the samples torrefied at 250 °C (Figure 4 e and 5 e) verify our assumption based on the DTG curve; that the decomposition of the remaining part of hemicellulose takes place in the temperature range of cellulose decomposition.

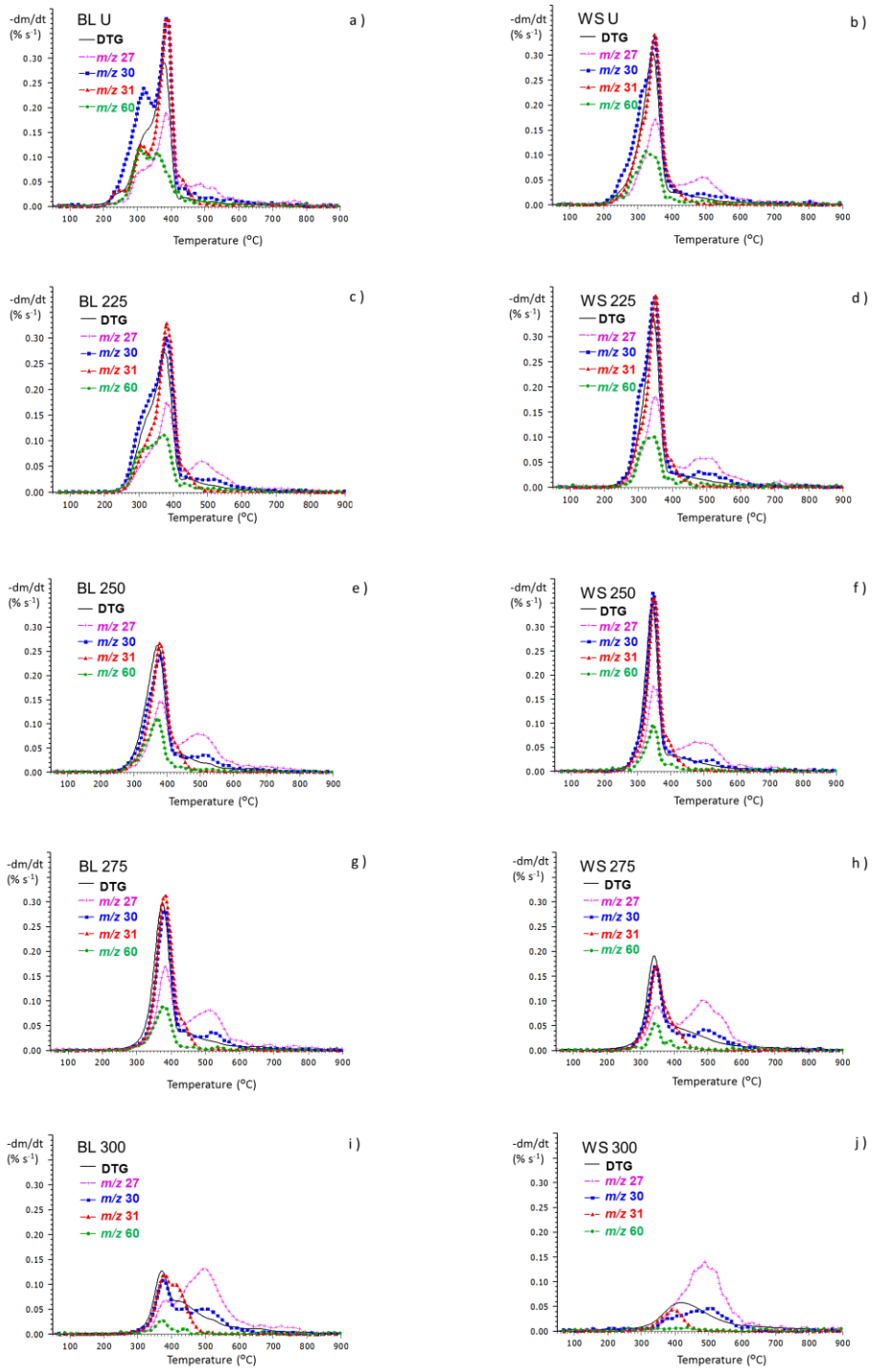

Figure 5. DTG curves and the evolution of a few characteristic organic products and fragments from black locust wood and wheat straw. (*m/z* 27, $C_2H_3^+$; *m/z* 30, formaldehyde; *m/z* 31, CH_3O^+; *m/z* 60, acetic acid and hydroxyacetaldehyde)

The main thermal decomposition product of cellulose is levoglucosan, which cannot be detected by TG/MS, but smaller decomposition products like hydroxyacetaldehyde (*m/z* 60), formaldehyde (*m/z* 30) and methanol (*m/z* 31, which is also a fragment ion of hydroxyacetaldehyde) can be monitored (Figure 5). Significant amounts of water and carbon dioxide are released during cellulose decomposition as well (Figure 4). The ion intensities describing the decomposition of cellulose (in the temperature range of the main DTG peak) do not decrease due to the thermal treatment up to 250 °C torrefaction temperature. Increasing the temperature of the torrefaction to 275 °C results in the reduced evolution of all cellulose decomposition products by about 40% in the wheat straw sample, while it does not decrease significantly in case of the black locust sample. This observation shows the more developed degradation of the cellulose in herbaceous wheat straw at 275 °C. After torrefaction at 300°C the ion intensity curves of the black locust sample (Figure 4 i and 5 i) show significant, but not complete degradation of cellulose, while in case of the wheat straw sample (Figure 4 j and 5 j) the ion curves prove the almost complete degradation of cellulose and hemicellulose. These TG/MS results confirm the results of the compositional analysis (Figure 1).

The evolution profile of methane (*m/z* 16 in Figure 4) shows a wide bimodal shape. In the temperature range of 370-500 °C methane forms during the thermal decomposition of lignin by the scission of the methoxy groups.[33] The slightly higher methane evolution from black locust in this temperature range is in accordance with the higher methoxy group content of the hardwood lignin comparing to the herbaceous lignin. After torrefaction, the relative amount of lignin increased in the samples due to the release of extractives, as well as to the degradation of hemicellulose and cellulose at higher torrefaction temperatures. The increased evolution of methane originating from the decomposition of lignin indicates this process. This effect is more pronounced in case of the wood

sample. In the temperature range of 400-600 °C, the evolution of small hydrocarbon molecules were observed, represented by the *m/z* 27 ion curves in Figure 5. The relative intensity of the hydrocarbon evolution is increasing by the torrefaction temperature in case of both the wood and straw samples. These hydrocarbon molecules may be produced by secondary reactions involving the decomposition products of cellulose, hemicellulose and lignin.

Methane formation above 500 °C and hydrogen evolution (*m/z* 2 in Figure 4) above 600 °C occur during the charring reactions. Comparing the intensities of the selected ions as a function of the torrefaction temperature, it can be observed that the evolution of hydrogen and methane are increasing, while the intensities of the other presented lignocellulose decomposition products are decreasing with raising the torrefaction temperature. These changes indicate the progress of the thermal decomposition during the torrefaction. In case of the black locust sample the ion intensity curve of carbon dioxide has two small sharp peaks, at 530 °C and 670 °C, indicating the presence of calcium oxalate, which originates from the bark of black locust wood.

3.6 Principal component analysis based on the TG/MS data. PCA has been applied to find further correlations between the ion intensity data of the main decomposition products obtained by TG/MS technique. The integrated intensities of the characteristic mass spectrometric ion curves have been used in the PCA calculation (Figure 6). The first principal component (Factor 1) describes 79.67% of the total variance of the TG/MS data, while the second and third principal components (Factor 2 and Factor 3) describe 11.56% and 3.19% of the total variance, respectively. The first principal component differentiates the untreated and lightly torrefied samples from the mildly and severely torrefied samples so Factor 1 correlates with the torrefaction temperature (Figure 6 a). The loading plot for Factor 1 and Factor 2 (Figure 6 b) reveals that mainly organic molecules contribute to Factor 1. The increasing torrefaction temperature correlates with the methane and hydrogen yields, which

shows that the severely torrefied samples produced more gases during the charring reactions. On the other hand, the decreasing torrefaction temperature correlates mainly with the formaldehyde, acetone and acetic acid formation since these compounds were released apparently during light and mild torrefaction, hence their pyrolytic yield is decreasing with increasing torrefaction temperature. The amounts of CO, CO_2, and water play the most important role in determining the second principal component. As was seen earlier, more gaseous products and water vapor were released from the herbaceous plants than from the hardwood. These differences can be explained by the different alkali ion contents of the studied samples. The higher alkali ion content promotes the gas formation during torrefaction of wheat straw and rape straw via fragmentation. On the other hand, the depolymerization reactions are dominant during the torrefaction of black locust wood indicated by the higher yield of furfural (sum of *m/z* 95 and 96) and furanone (*m/z* 84), which contributes also to the second principal component. On the other hand, the loading plots (Figure 6 d) suggest that the yield of furanone, furfural, methanol (*m/z* 31) as well as acetic acid and hydroxyacetaldehyde (*m/z* 60) also play a role in determining the third principal component. At the given torrefaction temperatures, the yields of these compounds are higher during the decomposition of black locust wood than of wheat straw and rape straw. The second and third principal components may be attributed to the effect of both the different chemical composition and the inorganic contents of the studied samples.

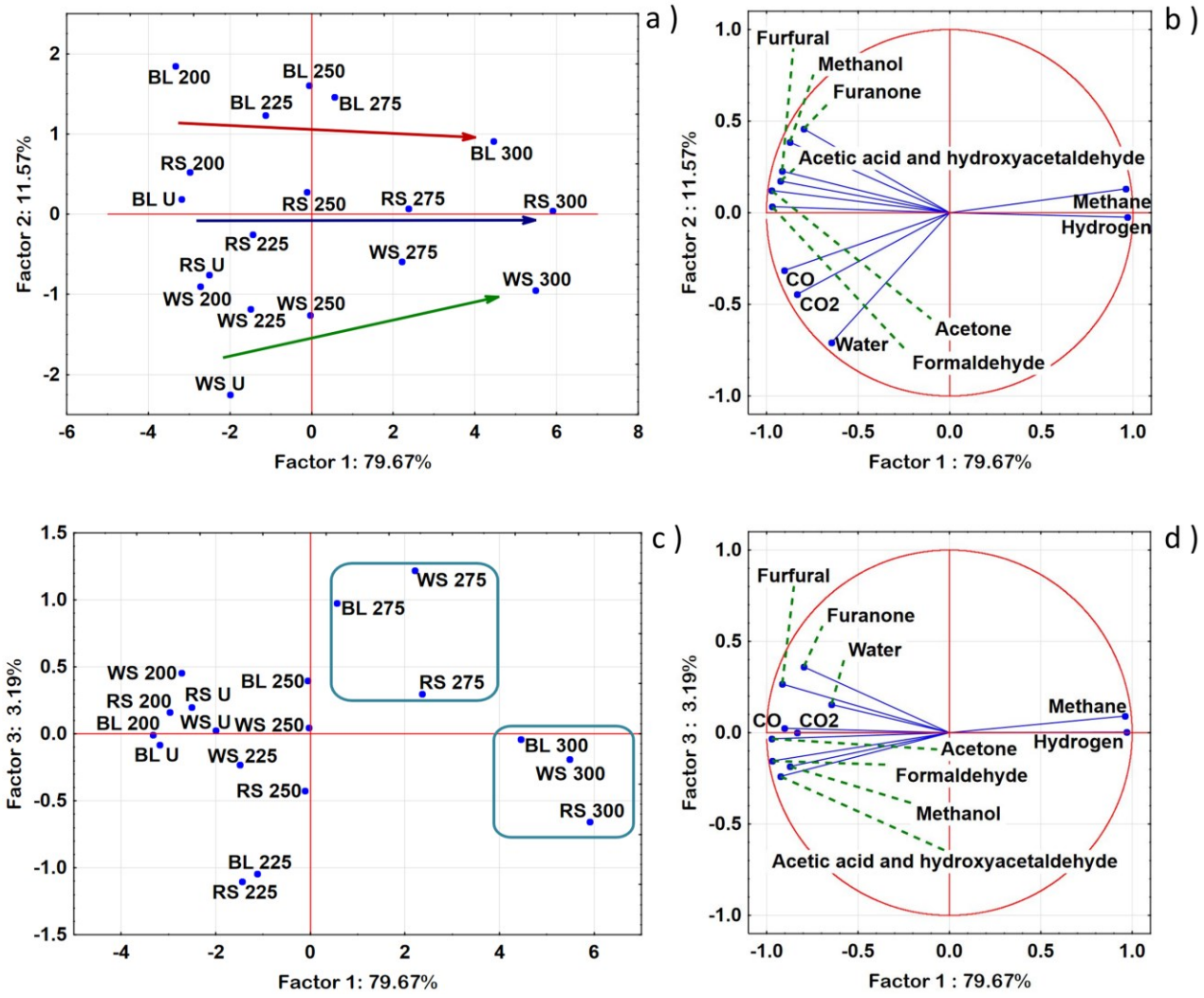

Figure 6. Principal component analysis (a, c) score and (b, d) loading plots based on TG/MS data. The score plots (a, c) represent the samples in the space defined by the Factors. Factor loadings (b, d) show the correlation between the original variables and the Factors.The arrows show the direction of the variation of the samples with increasing torrefaction temperature. WS: wheat straw, RS: rape straw, BL: Black locust wood

4. CONCLUSIONS

Comprehensive compositional analysis of untreated and torrefied wood and herbaceous samples has been performed with the goal of understanding deeper the thermal degradation processes taking place during torrefaction. The hemicellulose, cellulose and Klason-lignin contents of native and torrefied samples were determined after acidic hydrolysis. TG/MS was applied to provide further information about the composition of the samples by breaking down the macromolecules into smaller building blocks. The joint interpretation of the changes in the chemical composition, thermal stability and evolution profiles of typical lignocellulose decomposition products as a result of the thermal treatment revealed new information about the thermal degradation of the lignocellulose materials.

The extractable compounds evaporate at the beginning of the torrefaction; the volatile extractives disappeared from the samples torrified at 225 °C. The main mass of the hemicellulose content of each wood and herbaceous sample was thermally stable during 1 hour of torrefaction at 225 °C; however, changes in the evolution pattern of acetic acid indicate the scission of the most labile acetate groups from the hemicellulose chains at this temperature. About 40% of the hemicellulose content decomposes at 250 °C in case of black locust wood, and rape and wheat straw samples as well. The thermal decomposition of hemicellulose after mild thermal treatment shifted to higher temperature, indicating the modified structure of the torrefied hemicellulose. No significant difference was found in the thermal stability of straw and wood samples in spite of the large difference in the contents of inorganic materials. Therefore, it can be concluded that the thermal stability of hemicellulose is not influenced by the inorganic content of the sample contrary to cellulose, where the significant catalytic effect of the alkali ions on the thermal decomposition is a well-known phenomenon. The hemicellulose content of each sample torrefied at 275 °C is strongly reduced.

The degree of cellulose decomposition at 275 °C torrefaction temperature is significant only for herbaceous samples, while cellulose is not degraded in the wood sample at this temperature. The gradual increase in the amount of the acid insoluble materials indicates that the scission of the functional groups is accompanied by the enhanced formation of the cross-linked carbonaceous residues with increasing torrefaction temperature. The results of the proximate and ultimate analysis, HHV values, compositional analysis data and TG/MS experiments all clearly demonstrate the progress of the thermal decomposition during torrefaction in the temperature range of 200-300 °C. Statistical correlations have been found between the torrefaction temperature, chemical composition and TG/MS data of the untreated and torrefied samples using principal component analysis. Three sets of PCA calculations were undertaken using different types of data, which resulted in consistent results; the untreated and mildly torrefied samples were separated from the severely torrefied samples. The calculations revealed that the chemical composition and therefore the thermal properties have changed to a much greater extent in the temperature range of 275-300 °C than at lower torrefaction temperatures.

5. ACKNOWLEDGEMENT

This work is dedicated to the memory of Prof. Michael J. Antal, Jr. who contributed to the long-term co-operation in the field of biomass research between the Norwegian and Hungarian groups.

The authors are grateful to the NKFIH for financing the KTIA_AIK_12-1-2012-0014, TÉT_13_DST-1-2014-0003, OTKA PD-108389 and OTKA K119441 projects and to the “Bolyai János” research fellowship.

SINTEF acknowledge the financial support by the Research Council of Norway and a number of industrial partners through the projects BioCarb+ and GAFT.

6. SUPPORTING INFORMATION

Principal component analysis has been performed to find statistical correlations between the solid yields, the energy contents and the proximate and ultimate analysis data (Table 1). The PCA results can be found in Figure S1 in the supporting information.

7. REFERENCES

(1) Jakab E. Analytical Techniques as a Tool to Understand the Reaction Mechanism, Chapter 3 in *"* Recent Advances in Thermo-chemical Conversion of Biomass*" (*Eds. A. Pandey, T. Bhaskar, M. Stocker & R. Kumar Sukumaran) *Elsevier*, **2015**, pp. 73-106.

(2) Van der Stelt, M. J. C.; Gerhauser, H.; Kiel, J. H. A.; Ptasinski, K. J. *Biomass Bioenergy* **2011**, *35*, 3748-3762.

(3) Vu Bach, Q.; Skreiberg, Ø. *Renew. Sustain. Energy Rev.* **2016**, *54*, 665-677.

(4) Boateng, A. A.; Mullen, C. A. *J. Anal. Appl. Pyrolysis* **2013**, *100*, 95-102.

(5) Chang, S.; Zhao, Z.; Zheng, A.; He, F.; Huang, Z.; Li, H. *Energy Fuels* **2012**, *26*, 7009-7017.

(6) Prins, M. J.; Ptasinski, K. J.; Janssen, F. J .J. G. *J. Anal. Appl. Pyrolysis* **2006**, *77*, 35-40.

(7) Kim, Y. H.; Lee, S .M.; Lee, H. W.; Lee, J. W. *Biores. Technol.* **2012**, *116*, 120-125.

(8) Via B. K.; Adhikari, S; Taylor, S. *Biores. Technol.* **2013**, *133*, 1-8.

(9) Budai, A.; Wang, L.; Grønli, M.; Strand, L. T.; Antal, M. J.; Abiven, S.; Dieguez-Alonso, A.; Anca-Couce, A.; Rasse, D. P. *J. Agric. Food Chem.* **2014**, *62*, 3791-3799.

(10) Joshi, Y.; Di Marcello, M.; Krishnamurthy, E.; de Jong, W. *Energy Fuels* **2015**, *29* (8), 5078-5087.

(11) Di Blasi, C.; Branca, C.; Galgano, A.; Gallo, B. *Energy Fuels* **2015**, *29* (4), 2514-2526.

(12) Satpathy, S. K.; Tabil, L. G.; Meda, V.; Naik, S. N.; Prasad, R. *Fuel* **2014**, *124*, 269-278.

(13) Chen, Y.; Yang, H.; Yang, Q.; Hao, H.; Zhu, B.; Chen, H. *Bioresour. Technol*. **2014**, *156*, 70-77.

(14) Bilgic, E.; Yaman, S.; Haykiri-Acma, H.; Kucukbayrak, S. *Fuel Process. Technol*. **2016**, *144*, 197-202.

(15) Pronyk, C.; Mazza, G. *Bioresour. Technol*. **2012**, *106*, 117-124.

(16) Shoulaifar, T. K.; DeMartini, N.; Willför, S.; Pranovich, A.; Smeds, A. I.; Virtanen, T. A. P.; Maunu, S. L.; Verhoeff, F.; Kiel, J. H. A; Hupa, M. *Energy Fuels* **2014**, *28* (6), 3863-3872.

(17) Nhuchhen, D. R.; Basu, P.; Acharya, B. *Energy Fuels* **2016**, *30* (2), 1027-1038.

(18) Mišljenović, N.; Vu Bach, Q.; Tran, K. Q.; Salas-Bringas, C.; Skreiberg, Ø. *Energy Fuels* **2014**, *28* (4), 2554-2561.

(19) Tapasvi, D.; Khalil, R.; Skreiberg, Ø.; Tran, K. Q.; Grønli, M. *Energy Fuels* **2012**, *26* (8), 5232-5240.

(20) Li, T.; Geier, M.; Wang, L.; Ku, X.; Guell, B. M.; Løvas, T.; Shaddix, C. R. *Energy Fuels* **2015**, *29*, 177-184.

(21) Joshi, Y.; Di Marcello, M.; de Jong, W. *J. Anal. Appl. Pyrolysis* **2015**, *115*, 353-361.

(22) Pushkin, S. A.; Kozlova, L. V.; Makarov, A. A.; Grachev, A. N.; Gorshkova, T. A. *J. Anal. Appl. Pyrolysis* **2015**, *116*, 102-113.

(23) DeGroot, W. F.; Shafizadeh, F. *J. Anal. Appl. Pyrolysis* **1984**, *6*, 217-232.

(24) Sekiguchi, Y.; Shafizadeh, F. *J. Appl. Polym. Sci.* **1984**, *29*, 1267-1286.

(25) Várhegyi, G.; Antal, M. J.; Székely, F.; Till, F.; Jakab, E. *Energy Fuels* **1988**, *2*, 267-272.

(26) Khelfa, A.; Finqueneisel, G.; Auber, M.; Weber, J. V. *J. Therm. Anal. Calorim.* **2008**, *92*, 795-799.

(27) Dobele, G.; Rossinskaja, G.; Dizhbite, T.; Telysheva, G.; Meier, D.; Faix, O. *J. Anal. Appl. Pyrolysis* **2005**, *74*, 401-405.

(28) Torri, C.; Lesci, I. G.; Fabbri, D. *J. Anal. Appl. Pyrolysis* **2009**, *84*, 25-30.

(29) Shoulaifar, T. K.; DeMartini, N.; Karlström, O.; Hupa, M. *Fuel* **2016**, *165*, 544-552.

(30) Saleh, S. B.; Hansen, B. B.; Jensen, P. A.; Dam-Johansen, K. *Energy Fuels* **2013**, *27* (12), 7541-7548.

(31) Sebestyén, Z.; May, Z.; Réczey, K.; Jakab, E. *J. Therm. Anal. Calorim.* **2011**, *105*, 1061-1069.

(32) Jakab, E.; Faix, O.; Till, F.; Székely, T. *J. Anal. Appl. Pyrolysis* **1993**, *25*, 185-94.

(33) Jakab, E.; Faix, O.; Till, F. *J. Anal. Appl. Pyrolysis* **1997**, *40-41*, 171-86.

(34) Jensen A.; Dam-Johansen K.; Wójtowitz M. A.; Serio M. A. *Energ. Fuel* **1998**, 12, 929-938.

(35) Buryan, P.; Staff, M. *J. Therm. Anal. Calorim.* **2008**, *93*, 637-640.

(36) Mészáros, E.; Jakab, E.; Várhegyi, G.; Tóvári, P. *J. Therm. Anal. Calorim.* **2007**; *88*, 477-482.

(37) Mészáros, E.; Jakab, E.; Várhegyi, G.; Szepesváry, P.; Marosvölgyi, B. *J. Anal. Appl. Pyrolysis* **2004**, *72*, 317-328.

(38) Streibel, T.; Geissler, R.; Saraji-Bozorgzad, M.; Sklorz, M.; Kaisersberger, E.; Denner, T.; Zimmermann, R. *J. Therm. Anal. Calorim*. **2009**, *96*, 795-804.

(39) Streibel ,T.; Fendt, A.; Geissler, R.; Kaisersberger, E.; Denner, T.; Zimmermann, R. *J. Therm. Anal. Calorim.* **2009**, *97*, 615-619.

(40) (24) Mothe, C. G.; de Miranda, I. C. *J. Therm. Anal. Calorim.* **2009**, *97*, 661-665.

(41) (25) Souza, B. S.; Moreira, A. P. D.; Teixeira, A. M. F. R. *J. Therm. Anal. Calorim.* **2009**, *97*, 637-642.

(42) Sluiter, A.; Hames, B.; Ruiz, R.; Scarlata, C.; Sluiter, J.; Templeton, D.; Crocker, D. Laboratory analytical procedure, National Renewable Energy Laboratory, **2008**

(43) Sluiter, A.; Hames, B.; Ruiz, R.; Scarlata, C.; Sluiter, J.; Templeton, D. Determination of ash in biomass. Laboratory analytical procedure, National Renewable Energy Laboratory, Golden, CO. 2008

(44) Wold, S.; Esbensen, K; Geladi, P. *Chemom. Intell. Lab.Syst.* **1987**, 2, 37–52.

(45) Jakab, E.; Faix, O.; Till, F.; Székely, T. *J. Anal. Appl. Pyrolysis* **1995**, *35*, 167-179.

(46) Mészáros, E.; Jakab E.; Várhegyi G. *J. Anal. Appl. Pyrol*. **2007**, *79*, 61-70